ISSN 2543-9901

JOURNAL OF CASTING & MATERIALS ENGINEERING

AGH UNIVERSITY OF KRAKOW
FACULTY OF FOUNDRY ENGINEERING

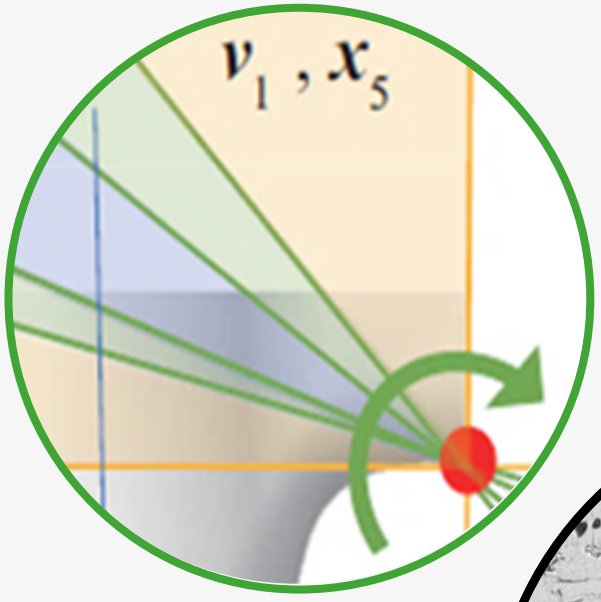

QUARTERLY
Vol. 7 No. 1/2023

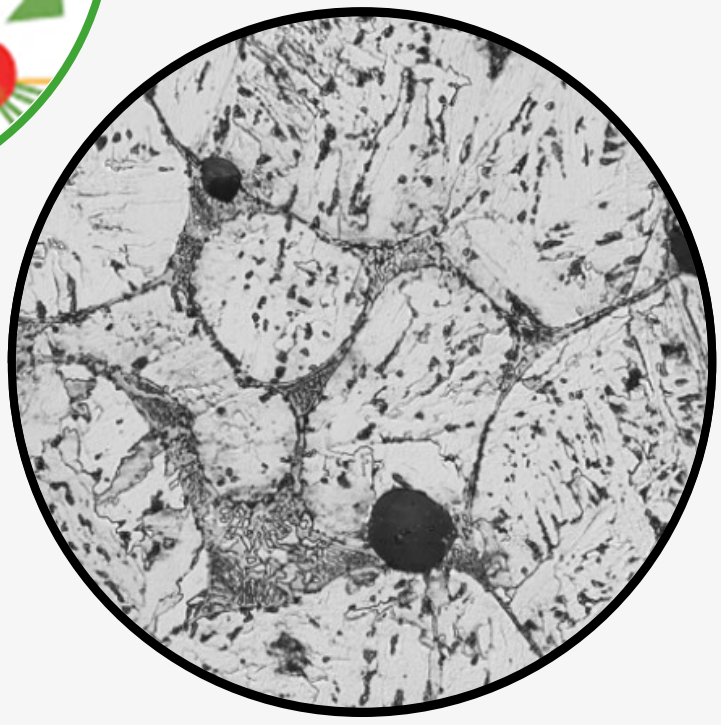

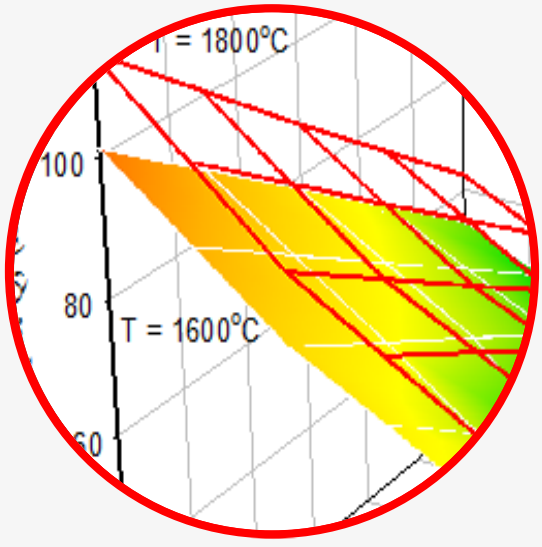

JCME

AGH UNIVERSITY PRESS
KRAKOW 2023

The articles published in the Journal of Casting & Materials Engineering have been given a favorable opinion by the rewievers designated by the Editorial Board.

www:
https://journals.agh.edu.pl/jcme/

AGH UNIVERSITY PRESS KRAKOW 2023

Wydawnictwa AGH (AGH University Press)
al. A. Mickiewicza 30, 30-059 Kraków
tel. 12 617 32 28, 12 638 40 38
e-mail: redakcja@wydawnictwoagh.pl
http://www.wydawnictwa.agh.edu.pl

Contents

Journal of Casting & Materials Engineering Vol. 7 No. 1 (2023) 1–8
https://doi.org/10.7494/jcme.2023.7.1.1

Effect of Particle Size of a Powder upon the Properties and Microstructure of Boron-modified Fe-Ni-Mo-Cu Sinters

Joanna Karwan-Baczewska[a], Małgorzata Perek-Nowak[a]*, Magdalena Majchrowska[a], Mario Rosso[b]

[a] AGH University of Krakow, al. A. Mickiewicza 30, 30-059 Krakow, Poland
[b] Politecnico di Torino, Corso Duca degli Abruzzi, 24, 10129 Torino TO, Italy
[*] *e-mail:* mperek@agh.edu.pl

Received: 11 October 2022/Accepted: 31 January 2023/Published online: 30 March 2023
This article is published with open access at AGH University of Science and Technology Journals

Abstract

The article discusses the effect of different particle fractions of prealloyed iron powder on the microstructure, density and hardness of sintered material. Each particle fraction (apart from 160–200 μm, which is a trace fraction) was modified with boron, its contents being, respectively, 0.2 wt.%, 0.4 wt.% and 0.6 wt.%. Next, the powder mixtures were pressed under a pressure of 600 MPa, and the final compacts were subject to sintering at 1200°C for 60 min in a hydrogen atmosphere. It was observed that the higher values of density and hardness were found in samples made from finer fractions of powder. A higher homogeneity of the microstructure and the highest degree of compactness was obtained in sinters from powder of 40–56 μm particle size, with 0.4 wt.% B. Due to the use of small particle fractions of prealloyed powder, a higher degree of compactness in sinters was obtained with lower boron content. Also indicated was which particle fraction of Fe-Ni-Mo-Cu powder should be applied to obtain density in sinters with boron addition equal to almost 100% of the relative density of the analyzed alloy. The presented studies have both scientific and technological aspects.

Keywords:

processing, powder metallurgy, Distaloy SA powder, activated sintering, particle fraction

1. INTRODUCTION

Powder metallurgy is a technology aiming at the production of bulk parts without reaching melting temperature, which in the case of iron mixtures is usually well above 1000°C. Thus, it provides the opportunity to introduce elements and compounds with high melting points, as well as controlling the distribution of these phases. However, in order to successfully proceed in producing a bulk material from an iron-containing powder or powder mixture, there is a need for a liquid phase during sintering. It was observed by Madan and German [1] that boron addition acts sufficiently well as a liquid-forming element, improving sintering by lowering its temperature and forming eutectic regions on the inter-particle boundaries. An explanation of the sintering mechanism for Fe-based alloys can be found in [2–7]. The thermodynamic approach, including regions of phase diagrams where various borides can be formed, are presented in [7, 8].

The formation of the eutectic regions in the sintered samples plays also an important role in decreasing porosity which may increase mechanical properties. The effect of porosity on mechanical properties in Fe-Mo-Ni alloys in tensile and fatigue tests is described in [9]. The addition of boron to iron based sinters (Fe-Mo-B) results in a change in the deformation behavior from ductile to brittle with the increase of boron content [10]. It was found that boron activates a sintering process through a liquid phase formation as a result of a reaction between matrix elements (Fe, Mo, Ni) and borides of the $(Fe, Mo, Ni)_2B$ type [4, 5, 7]. In alloys containing a sufficient amount of boron, the liquid phase may form as quickly as 1176°C. The amount of the liquid phase is affected by copper which may decrease the temperature of the liquid phase formation [7]. Both processes increase the consolidation level and mechanical properties of the sintered samples. It has been proven that the chemical composition of Distaloy SA powder allows one to obtain appreciably higher mechanical properties for sinters alloyed with a lower boron addition.

Additionally, to understand this sintering mechanism better, a dilatometric study brings valuable information. The dilatometric study upon heating and cooling of Fe-Mo-B sinters was presented in detail with respect to the composition of specimens and to a heating rate in [11]. This liquid sintering process increases the consolidation level and provides higher mechanical properties of the sintered samples. It has been proven that the chemical composition of the alloyed powders allows appreciably higher mechanical properties to be obtained [10, 12–18].

The mechanical properties of sintered steels with boron and borides were analyzed in [9–20]. In order to enhance the mechanical and surface properties, especially the hardness

and wear resistance of sintered alloys modified by boron, a heat and chemical treatment was applied [21, 22].

Moreover, applying finer particle fractions of alloyed powders makes it possible to acquire a higher consolidation level of sinters with a lower boron content. In this paper, the influence of different particle fraction of boron modified Fe-Ni-Mo-Cu powders on the density, hardness and microstructure of sintered samples was analyzed.

2. MATERIALS AND METHODS

A prealloyed Distaloy SA powder supplied by the Höganäs company with the composition Fe 1.75%Ni-1.5%Cu-0.5%Mo was used in the studies. The particle size of Distaloy SA powder (general particle fraction) is 20–180 μm. By means of screen analysis (PN-EN 24497, July 1999) using sieves with a mechanical shaker, the following particle fractions were determined and are listed in Table 1.

Table 1
Sieve analysis of Distaloy SA powder

Sieve size [μm]	Retained [%]	Cumulative mass retained [%]
160–200	0.11	0.11
100–160	25.21	25.32
71–100	29.63	54.95
63–71	7.63	62.58
56–63	3.54	66.12
40–56	19.70	85.82
< 40	14.18	100.00

Each particle fraction and a general one (20–180 μm) were modified with boron, respectively, and followed by mixing in a Turbula mixer for 15 minutes. The boron contents used in the studies were: 0.2 wt.%, 0.4 wt.% and 0.6 wt.%. It is worth noting here that 160–200 μm is a trace fraction, therefore it was not used in the further experiments. Additionally, boron-free samples were prepared for reference for each particle fraction. Five specimens were prepared for each composition and fraction. In the next step, powder mixes were pressed under 600 MPa in a mechanical press, and the final compacts were subjected to sintering. No pressure was imposed on samples during sintering. The sintering took place in a tube furnace at a temperature of 1200°C for 60 min in a hydrogen atmosphere as established in [8, 23].

In successive studies, the density of compacts and Distaloy powder sinters per each particle fraction were investigated. The density of compacts and sinters was determined by means of the Archimedes method (PE-EN ISO 2738, December 2001). Samples were polished using Struers polishing machine. A set of abrasive papers of grade 500 to 2000 was used. The final polishing was with a cloth with a 1 μm diamond paste followed by etching with a HNO_3 water solution. Additionally, hardness was measured with Brinell's method (PN-EN ISO 65060-1, 2002). Structural observations were performed with an optical microscope Neophot 32. The effect of particle effect exerted upon the density, hardness and microstructure of boron-modified Distaloy SA sinters was analyzed.

3. RESULTS AND DISCUSSION

3.1. Density of green compacts and sinters

The determined densities of compacts and sinters made from various particle fractions of Distaloy SA powder (Table 1) with boron additions are shown in Figure 1a, b. According to the analysis of the density measurements of compacts modified with boron, irrespective of the boron content and particle fractions of the Distaloy SA powders, the density values of green compacts do not change and are about 6.9 g/cm^3. An example of such measurements for two chosen fractions, general and 40–56 μm ones, are presented in Figure 1a, b. Instead, the densities of Distaloy SA sinters with boron additions showed that particle fractions substantially influenced the degree of compactness of the samples under investigation. In all of the particle fractions used, the degree of compactness increased as boron contents rose (0.2–0.6 wt.%).

a)

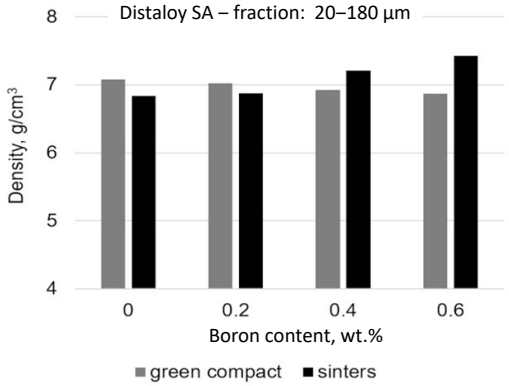

b)

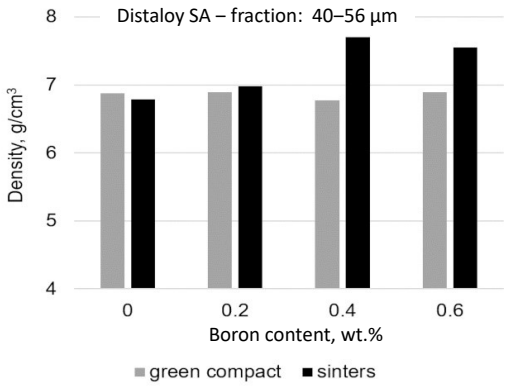

Fig. 1. Effect of particle fraction of powder and boron addition upon density of green compacts and sinters: a) 20–180 μm fraction; b) 40–56 μm fraction

The density of boron-free samples after pressing and sintering are comparable. The small drop of density is caused by the formation of smaller amounts of liquid phase based on copper (melting temperature 1084°C). On the other hand, in the case of lower boron contents (0.2 wt.% B), a thin layer of liquid eutectic is created at the particles' boundaries, which influences the raise of density. The liquid eutectic consists of (Fe, Ni, Mo)-complex borides [7]. However, with higher boron contents, a tendency toward higher densification of sinters

due to the larger amount of the liquid phase is observed [7]. This tendency is well illustrated in Figure 2.

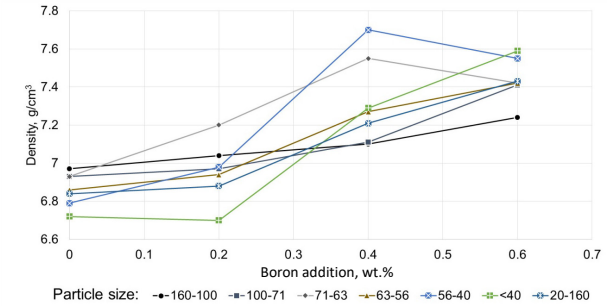

Fig. 2. Density of Distaloy SA sinters for all used powder fractions with boron addition in respect to particle fraction of powder

In the case of Distaloy SA sinters made based upon coarse fractions (100–160 μm, 71–100 μm, 63–71 μm, 56–63 μm) and general fraction (20–180 μm) with 0.6 wt.% B, lower densities were obtained if compared with sinters produced from fine fractions (40–56 μm and under 40 μm) with the same boron content (0.6 wt.% B) (Fig. 2).

During sintering the volume of samples decreases in relation to the green compacts. In the case of boron free sinters, the relative density is in a range of 85% to 89% for fraction under 40 μm and 100–160 μm, respectively. Due to addition of boron, the tendency is reversed and highest densities are achieved by finer powders; e.g. 99% and 98% for 40–56 μm fraction with 0.4 wt.% B or 0.6 wt.%, respectively.

The value of the relative density of Distaloy SA sinters with 0.6 wt.% B made from coarse fractions is 94% (fraction 100–160 μm) and 96% (fractions 71–100 μm, 63–71 μm and 56–63 μm and general fraction 20–180 μm); whereas, for fine fractions (40–56 μm and under 40 μm) – 98% (Tab. 2). In addition, it was observed that it is possible to get the highest densities at a lower boron level with decreasing particle size in sinters, viz. 0.4 wt.%. A conclusion from the analysis of the experiment results is that for each particle fraction used, the highest degree of compactness occurs at the increase in boron of contents from 0.2 wt.% to 0.4 wt.%. However, as the particle size of Distaloy SA diminishes at the same boron content of 0.4 wt.% B kept, the density values increase obtaining a value of 7.70 g/cm^3 in case of 40–56 μm fraction (Fig. 1b). Nevertheless, a sinter made from fraction with particle size lower than 40 μm and also with 0.4 wt.% B presents a slightly lower density of 7.29 g/cm^3, which corresponds to the relative density of 94% (Tab. 2, Fig. 2).

The highest relative densities were obtained for sinters from Distaloy powders SA, fractions 63–71 μm and 40–56 μm with 0.4 wt.% B (97% and 99%, see Table 2). The increase in density for increased boron contents from 0.4 to 0.6% is appreciably lower. The highest actual and relative density values for Distaloy SA sinters with 0.4 wt.% B were found for fine powders (viz. 40–56 μm and under 40 μm).

Table 2
Density of Distaloy SA sinters with boron addition in respect to particle fraction of powder [16]

Particle fraction [μm]	Boron [wt. %]	Theoretical density [g/cm^3]	Real density [g/cm^3]	Relative density [%]
100–160	0.0	7.93	6.97	89
	0.2	7.89	7.04	90
	0.4	7.85	7.10	91
	0.6	7.81	7.24	94
71–100	0.0	7.93	6.93	88
	0.2	7.89	6.97	89
	0.4	7.85	7.11	92
	0.6	7.81	7.41	96
63–71	0.0	7.93	6.93	88
	0.2	7.89	7.20	92
	0.4	7.85	7.55	97
	0.6	7.81	7.42	96
56–63	0.0	7.93	6.86	87
	0.2	7.89	6.94	89
	0.4	7.85	7.27	94
	0.6	7.81	7.42	96
40–56	0.0	7.93	6.79	86
	0.2	7.89	6.98	89
	0.4	7.85	7.70	99
	0.6	7.81	7.55	98
< 40	0.0	7.93	6.72	85
	0.2	7.89	6.70	86
	0.4	7.85	7.29	94
	0.6	7.81	7.59	98
20–180	0.0	7.93	6.84	87
	0.2	7.89	6.88	88
	0.4	7.85	7.21	93
	0.6	7.81	7.43	96

3.2. Hardness of sinters

While analyzing the results of hardness for boron-modified Distaloy SA sinters vs. particle size of Distaloy SA powder, it was found that irrespective of the used fraction, as boron content in the samples under investigation increases, their hardness will also increase. Additionally, it was observed that the highest average hardness was obtained for the finest fractions, viz. 40–56 μm (145 HB at 0.2 wt.% B, 190 HB at 0.6 wt.% B, see Fig. 3) and under 40 μm (152 HB at 0.2 wt.% B, and 223 HB at 0.6 wt.% B, see Fig. 3).

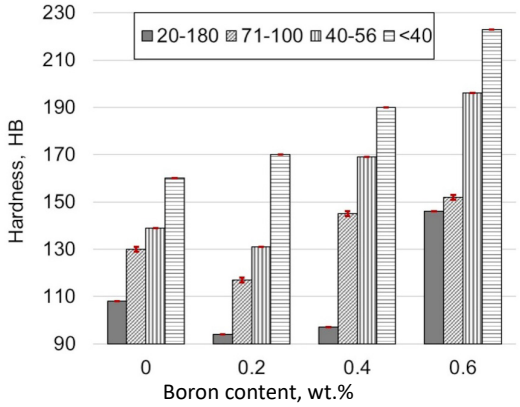

Fig. 3. Effect of powder particle fractions and boron contents upon the hardness of prepared sinters: fraction 20–180 μm, 71–100 μm, 40–56 μm, and < 40 μm

It should be also underlined that sinters, made from the fraction under 40 μm are characterized with appreciably higher hardness irrespective of boron contents; for example: sinters from general fraction (20–180 μm) with 0.2 wt.% and 0.6 wt.% B have the following average hardness values: 130 and 160 HB (Fig. 3). Distaloy sinters made from general fraction (20–180 μm) have appreciably lower hardness values than sinters from undersized fraction (Fig. 3). So, the hardness value of sinters under investigation depends on boron contents and particle size (Fig. 3). As the Distaloy SA particle size decreases, and boron contents increase, the hardness values in sinters under examination were considerably higher. The hardness of Distaloy SA sinters depends on their degree of compactness and the particle size of Distaloy SA powder used – the finer the particle fraction, the higher the density and hardness of the prepared sinters (Tab. 2, Fig. 3).

3.3. Microstructure observations of sinters

Microscopic observations of boron-modified Distaloy SA sinters showed that irrespective of the particle fraction of the powder used, the microstructure consists of an iron matrix with a solidified, non-homogeneous eutectic mixture visible upon iron particles boundaries. In addition, precipitates of fine borides were noticed in the ferrite matrix.

On the other hand, porosity seems to quite noticeable in boron-free samples (Figs. 4a, 5a, 6a, and 7a) and also in the samples with lowest boron content (Figs. 4b, 5b, 6b, and 7b).

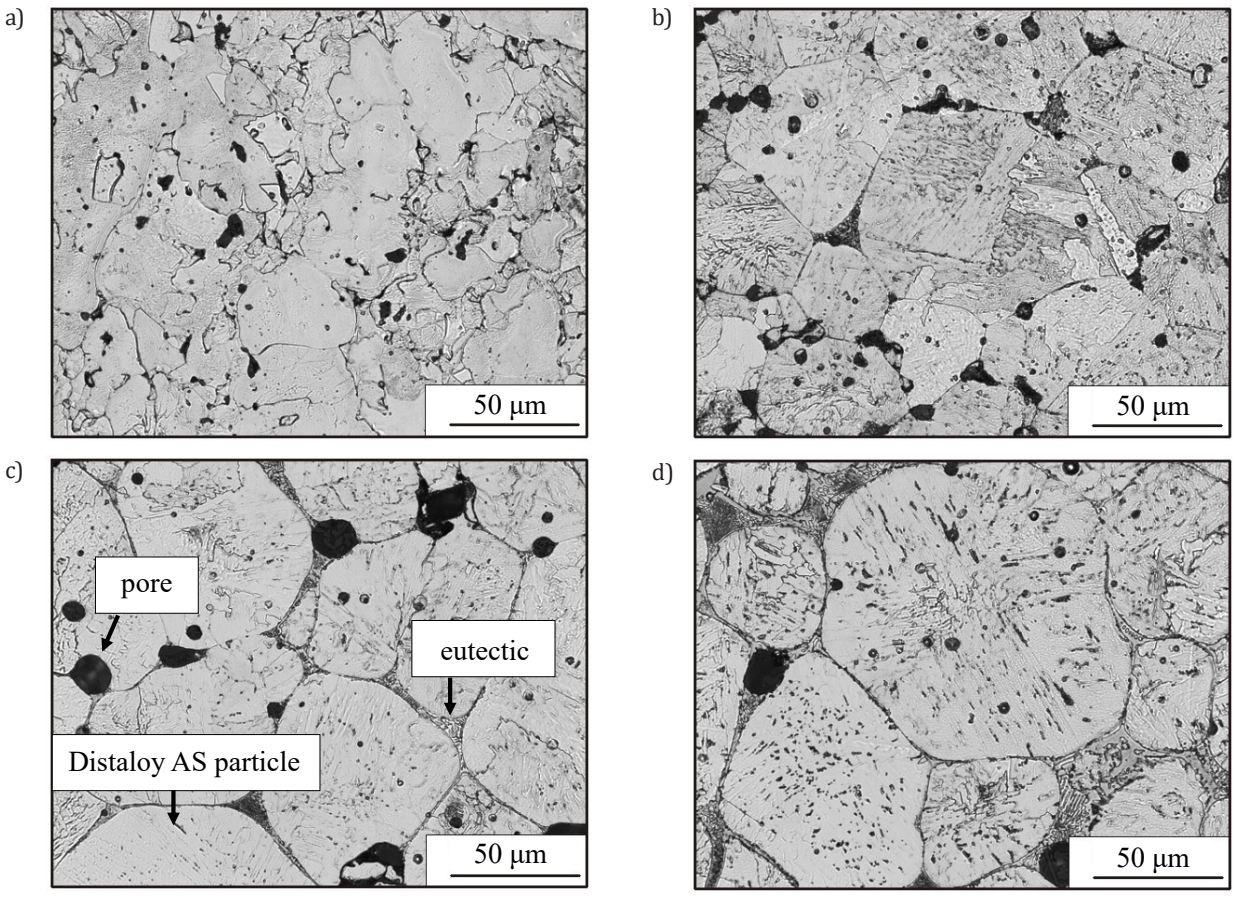

Fig. 4. Microstructure of Distaloy SA sinters alloyed by boron for 20–180 μm particle fraction: a) 0.0 wt.% B; b) 0.2 wt.% B; c) 0.4 wt.% B; d) 0.6 wt.% B [7]

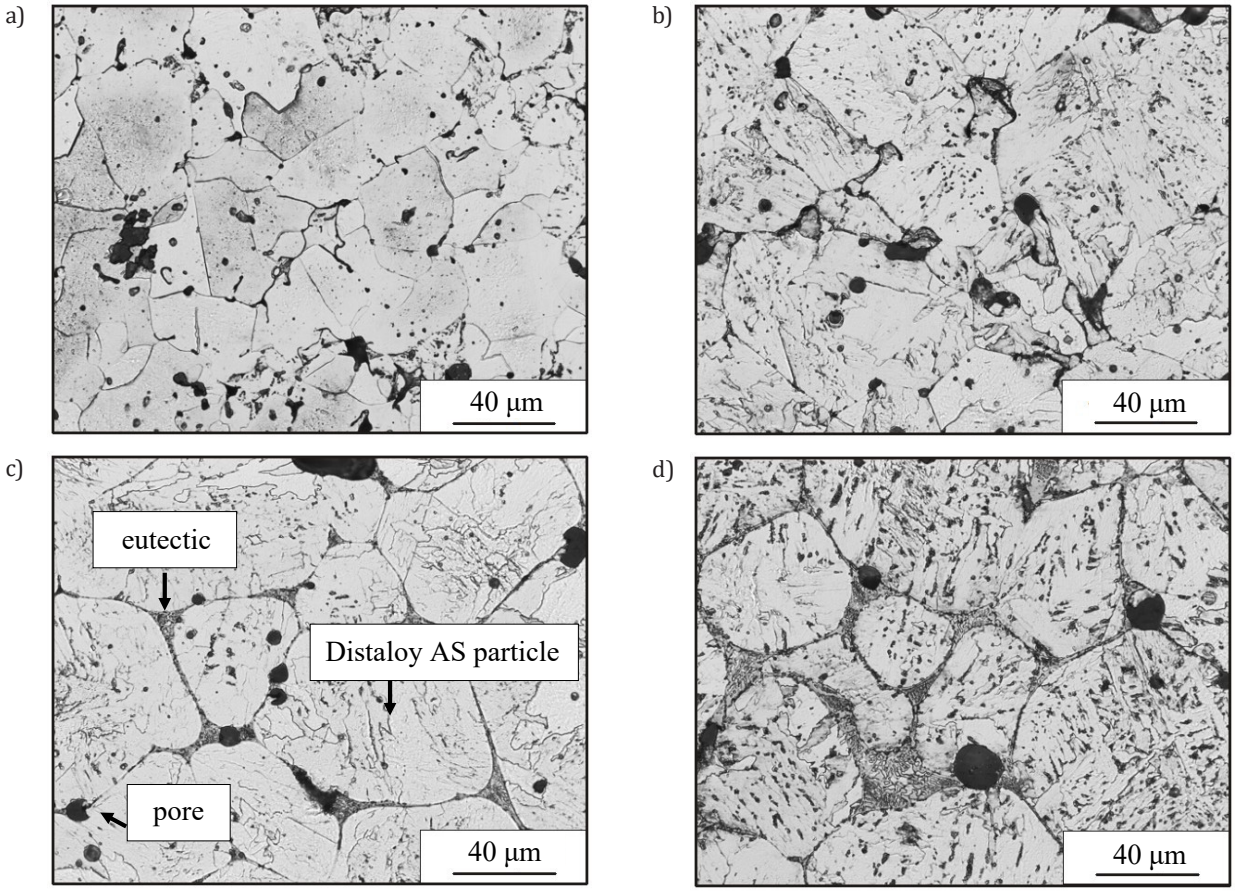

Fig. 5. Microstructure of Distaloy SA sinters alloyed by boron for 70–100 µm particle fraction: a) 0.0 wt.% B; b) 0.2 wt.% B; c) 0.4 wt.% B; d) 0.6 wt.% B

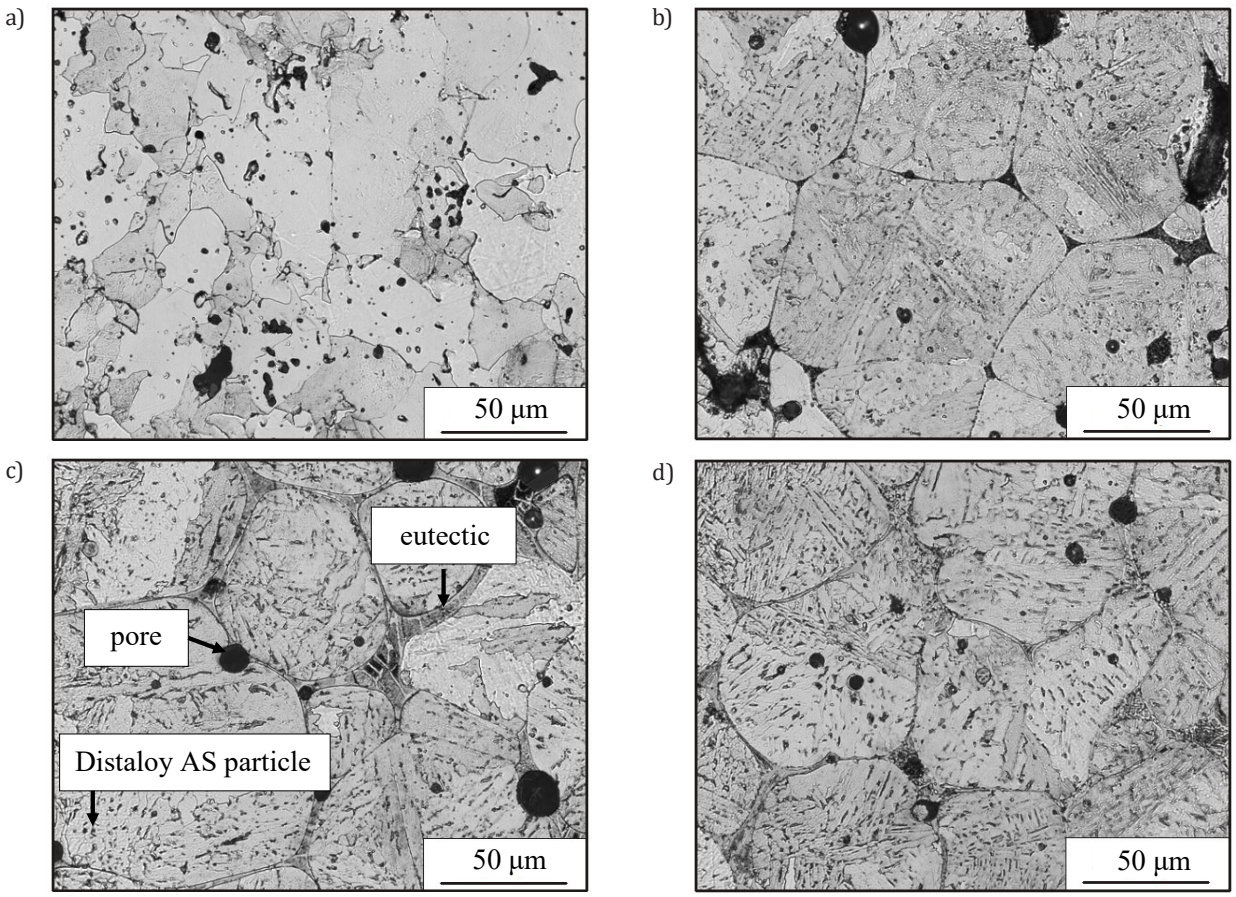

Fig. 6. Microstructure of Distaloy SA sinters alloyed by boron for 40–56 µm particle fraction: a) 0.0 wt.% B; b) 0.2 wt.% B; c) 0.4 wt.% B; d) 0.6 wt.% B

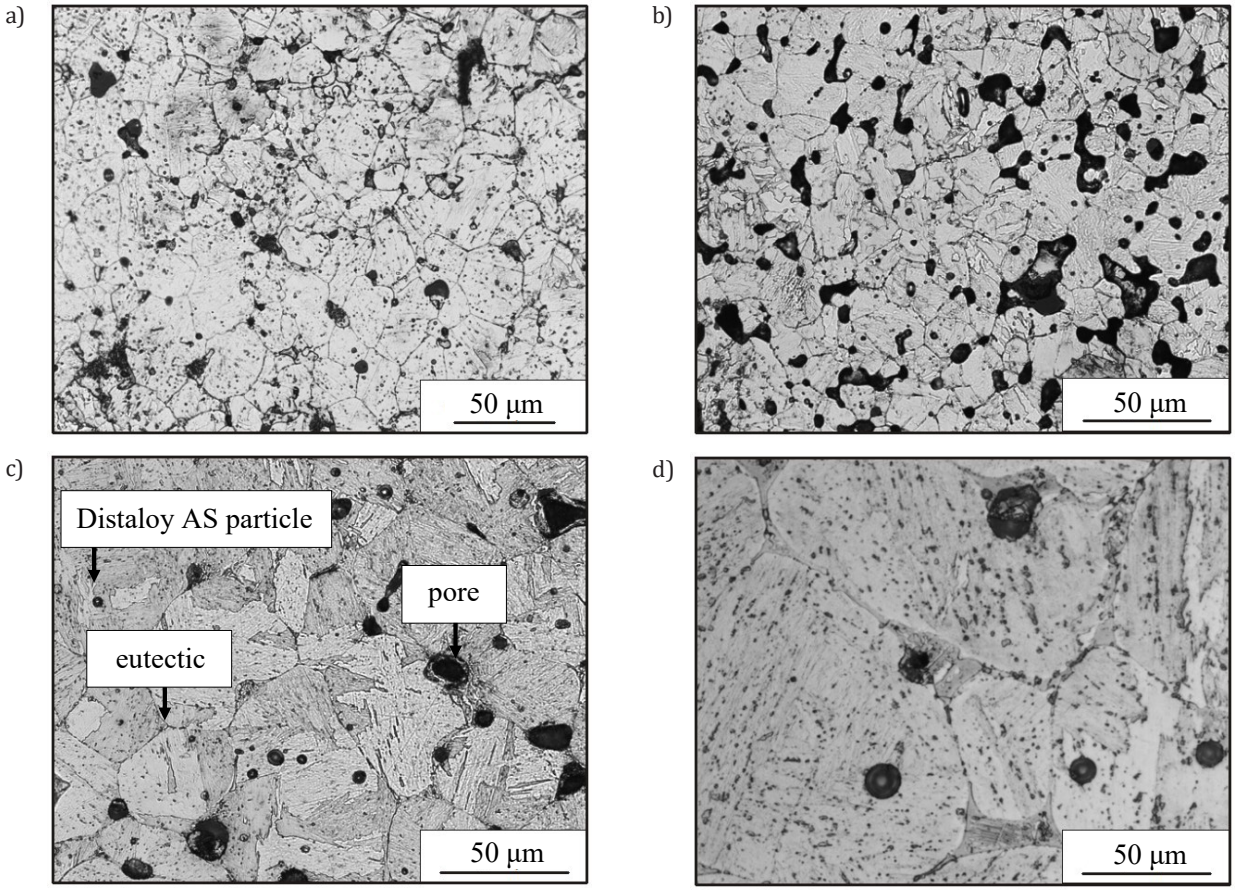

Fig. 7. Microstructure of Distaloy SA sinters alloyed by boron for <40 μm particle fraction: a) 0 wt.% B; b) 0.2 wt.% B; c) 0.4 wt.% B; d) 0.6 wt.% B

A small number of pores occurs in the microstructure of sinters under observation with higher boron content (0.4 wt.% and 0.6 wt.%) (Figs. 4c, d; 5c, d; 6c, d, and 7c, d). Thus, in general, one may say that the more eutectics is formed, the lower porosity. Those are only spheroidal pores, in particular in sinters produced from finer powder fraction: 40–56 μm and under 40 μm (Figs. 6 and 7).

As particle fractions in Distaloy SA powders decreased and boron contents increased, a smaller non-homogeneity of fine borides was observed in the microstructure of sinters under investigation – uniform precipitations of fine borides inside particles (Figs. 5c, d; 6c, d, and 7c, d) and more uniform precipitations of eutectics between particles boundaries, especially for fractions 40–56 μm and under 40 μm (Figs. 6d, 7d). In all microstructures observed, there was discernible increase of particle size with boron concentration – the bigger the particle, the higher the boron contents in sinters (Figs. 4–7). Thus, the formation of a large amount of the liquid phase favors the growth of particles at the expense of the smaller ones.

A characteristic feature for sintering Distaloy with boron is activated sintering resulting in the formation of eutectic containing Fe_2B and Fe_3B phases [7, 19]. In the microstructures of Distaloy SA sinters with 0.6 wt.% boron produced from a general fraction (20-180 μm) and from a coarse fractions (100–160 μm, 71–100 μm, 63–71 μm) larger quantities of eutectic phase located upon grain boundaries were observed (Fig. 3 and 4) than in the microstructures of sinters produced from fine fractions (56–63 μm, 40–56 μm and under 40 μm) (Figs. 6a and 7). Besides, no appreciable grain growth was noticed in the microstructures of sinters made from Distaloy SA powders of many fractions: 100–160 μm, 63–71 μm, 56–63 μm and 40–56 μm, modified with 0.4 wt.% and 0.6 wt.% B, which results from eutectic uniformly distributed upon grain boundaries (Figs. 4c, d; 5c, d; 6c, d). While using finer particle size, the sintering process enables the formation of larger amounts of liquid phase which in turn improves densification. The smaller the particles, the larger the specific surface and thus sintering is enhanced.

It should also be stressed that the highest values of real density (7.55 g/cm^3 and 7.70 g/cm^3) and relative density (about 97% and 99%) were noticed in Distaloy SA sinters produced from finer particle fractions viz. 63–71 μm and 40–56 μm with 0.4 wt.% B content.

The performed structural investigations showed that in sinters made from Distaloy SA powders of finer particle fractions (63–71 μm, 56–63 μm, 40–56 μm and under 40 μm), the non-homogeneity inside ferrite grains decreased as the boron contents increased. Additionally, uniformly distributed borides and an eutectic all along the grain boundaries were observed. The changes noticed in the microstructures of sinters under investigation influenced the degree of their compactness and hardness – they both increased (Figs. 3, 5–7).

It should also be underlined that a smaller non-uniformity of the microstructure and the highest degree of compactness can be obtained in sinters from Distaloy SA powder with 0.4 wt.% B, which belongs to 40–56 μm fraction. Due to the use of small grain fractions of Distaloy SA, one can obtain a higher degree of compactness in sinters and already at lower boron contents.

An additional scientific and technological achievement was the indication of the granular fraction of Distaloy SA powder in order to obtain almost 100% relative density of sinters from Distaloy SA powder with the addition of boron.

The experiments have shown that the application of Distaloy SA powder with a particle fraction of 40–56 μm allows a relative density of 99% to be obtained already at 0.4 wt.% B (Tab. 2) together with high hardness (Fig. 3). The structural investigations reveal, that in Distaloy SA sinters made from finer fractions (40–56 μm), borides are regularly distributed in the structure while eutectic regions are homogeneously distributed on the grain boundaries (Fig. 6).

The application of the given particle fraction of Distaloy SA powder with 0.4 wt.% B will significantly decrease the production costs of sintered elements due to implementing of conventional technologies of pressing and sintering allowing almost 100% relative density to be achieved, which in other cases can only be obtained by applying more expensive technologies of powder metallurgy (hot pressing, isostatic pressing, or finally SPS).

The described method of conventional pressing and sintering can be applied in the production of gearwheels with increased properties (density, hardness) on the basis of a given particle fraction of Distaloy SA powder with boron additions. Thus, the presented studies have both scientific and technological aspects.

4. CONCLUSIONS

The following conclusions were drawn from the research conducted and observations:

- It was observed that the density and hardness of the material depend strongly on the particle fraction of powder; with an increase in density, hardness also rises. Indeed, higher values of density and hardness were observed in samples made from the finer fraction of a Distaloy SA powder (especially 40–56 μm).
- A smaller non-uniformity of the microstructure and the highest degree of compactness can be obtained in sinters from the powder of fraction 40–56 μm, with 0.4 wt.% B.
- Due to the use of small particle fractions of prealloyed powder, a higher degree of compactness in sinters was obtained with lower boron contents.
- The hardness of sinters under investigation depends on boron contents and particle size.
- During sintering, the volume of samples decreases in relation to the green compacts.
- The liquid-phase enhances the sintering process for all fractions but it is the most visible in case of 40–56 μm fraction with 0.4 wt.% and 0.6 wt.% B giving 99 and 98% of relative density.

Acknowledgements

The financial support of AGH University of Science and Technology under statutory fund grant no. 16.16.180.006 is acknowledged.

REFERENCES

[1] Madan D.S. & German R.M. (1986). Enhanced sintering of iron alloyed with B, C, P, Mo, Ni. *Proceedings of International PM Conference, Germany, Düsseldorf*, 2, 1223–1226.
[2] German R.M., Hwang K.S. & Madan D.S. (1987). Analysis of Fe-Mo-B Sintered Alloys. *Powder Metallurgy International*, 19(2), 15–18.
[3] Sarasola M., Tojal C. & Castro F. (2004). Study of boron behavior during sintering of Fe/Mo/B/C alloys to near full density. *Euro PM2004 Conference Proceedings, Austria, Vienna 17–21.10.2004*, 3, 319–326.
[4] Sarasola M., Gómez-Acebo T. & Castro F. (2004). Liquid generation during sintering of Fe-3.5%Mo powder compacts with elemental boron addition. *Acta Materialia*, 52, 4615–4622. Doi: https://doi.org/10.1016/j.actamat.2004.06.018.
[5] Bolina R. & German R.M. (2004). Supersolidus sintering of boron doped stainless steel powder compacts. *EuroPM 2004, Austria, Vienna 17–21.10.2004*, 3, 341–348.
[6] Sarasola M., Gómez-Acebo T. & Castro F. (2005). Microstructural development during liquid phase sintering of Fe and Fe-Mo alloys containing elemental boron additions. *Powder Metallurgy*, 48(1), 59–67. Doi: https://doi.org/10.1179/003258905X37558.
[7] Karwan-Baczewska J. & Onderka B. (2017). Sintering prealloyed powders Fe-Ni-Cu-Mo Modified by boron base on thermodynamic investigations. In: L. Dobrzański (Ed.), *Powder Metallurgy – Fundamentals and Case Studies,* IntechOpen, 3, 29–53. Doi: http://dx.doi.org/10.5772/66875 .
[8] Dudrová E., Selecká M., Bureš R. & Kabátová M. (1997). Effect of boron addition on microstructure and properties of sintered Fe-1.5Mo powder materials. *ISIJ International*, 37(1), 59–64. Doi: https://doi.org/10.2355/isijinternational.37.59.
[9] Chawla N. & Deng X. (2005). Microstructure and mechanical behavior of porous sintered steels. *Materials Science and Engineering A,* 390(1–2), 98–112. Doi: https://doi.org/10.1016/j.msea.2004.08.046.
[10] Karwan-Baczewska J. (1996). Boron influence on the liquid phase sintering and mechanical properties of P/M Distaloy alloys. *Advanced Powder Metallurgy & Particulate Materials*, 3, (11-15)–(11-27).
[11] Molinari A., Gialanella S., Straffelini G., Pieczonka T. & Kazior J. (2000). Dilatometry study of the sinteringbBehavior of boron-alloyed Fe-1.5 pct Mo powder. *Metallurgical and Materials Transactions A,* 31, 1497–1506. Doi: https://doi.org/10.1007/s11661-000-0160-9.
[12] Toennes C., Ernst P., Meyer G. & German R.M. (1992). Full density sintering by boron addition in a martensitic stainless steel. *Advanced in Powder Metallurgy & Particulate Materials*, 3, 371–381.
[13] Nakamura M. & Kamada K. (1991). Influence of the addition of boron on the sintering temperature and the mechanical properties of P/M type stainless steels. *Journal of the Japan Society of Powder Metallurgy*, 38(1), 22–26. Doi: https://doi.org/10.2497/jjspm.38.22.
[14] Kuroki H.A. (2001). A review on the effect and behaviour of boron in sintered iron and steel. Journal of the Japan Society of Powder Metallurgy, 48(4), 293–304. Doi: https://doi.org/10.2497/jjspm.48.293.
[15] Karwan-Baczewska J. (2001). The properties and structure of boron modified P/M iron-molybdenum alloys. *Archives of Metallurgy*, 46(4), 439–445.
[16] Karwan-Baczewska J. (2008). *Spiekane stopy na bazie proszku żelaza modyfikowane borem* [Sintered alloys based on iron powder with boron]. Kraków: AGH Uczelniane Wydawnictwa Naukowo-Dydaktyczne.
[17] Karwan-Baczewska J. (2015). Processing and properties of Distaloy SA sintered alloys with boron and carbon. Archives Metallurgy and Materials, 60(1), 41–45. Doi: https://doi.org/10.1515/amm-2015-0006.
[18] Karwan-Baczewska J. (2011). The properties of Fe-Ni-Mo-Cu-B materials produced via liquid phase sintering. Archives Metallurgy and Materials, 56(3), 789–796. Doi: https://doi.org/10.2478/v10172-011-0087-8.

[19] Perek-Nowak M. & Karwan-Baczewska J. (2017). Elastic properties and structural observations of Distaloy SA powder sintered with boron and carbon. *Metallurgy and Foundry Engineering*, 43(2), 107–115. Doi: http://dx.doi.org/10.7494/mafe.2017.43.2.107.

[20] Sulima I., Jaworska L. & Karwan-Baczewska J. (2015). Effect of boron sinter-aid on the microstructure and properties of austenitic stainless steel-TiB2 composites. Archives Metallurgy and Materials, 60(4), 2619–2624. Doi: https://doi.org/10.1515/amm-2015-0423.

[21] Karwan-Baczewska J., Dymkowski T., Sobiecki J.R. & Formański T. (2010). Processing and surface properties of based on iron sintered alloys after plasma nitriding treatment. *Archives Metallurgy and Materials*, 55(2), 383–389.

[22] Karwan-Baczewska J. (2000). Influence of boron on the structure and mechanical properties of sintered and ion-nitrided distaloy alloys. *International Journal of Materials and Product Technology*, 15, 193–204. Doi: https://doi.org/10.1504/IJMPT.2000.001243.

[23] Karwan-Baczewska J. & Rosso M. (2001). Effect of boron on microstructure and mechanical properties of PM sintered and nitrided steels. *Powder Metallurgy*, 44(3), 221–227. Doi: https://doi.org/10.1179/003258901666374.

Journal of Casting & Materials Engineering Vol. 7 No. 1 (2023) 9–14
https://doi.org/10.7494/jcme.2023.7.1.9

Research on New Al-Ag-Mo Alloys Dedicated to Wire Applications in Overhead Power Lines

Justyna Grzebinoga[a*], Andrzej Mamala[a], Wojciech Ściężor[a], Radosław Kowal[a]

[a] AGH University of Krakow, Faculty of Non-Ferrous Metals, Mickiewicza 30 Ave, 30-059 Krakow, Poland
e-mail: jgr@agh.edu.pl

Received: 28 October 2022/Accepted: 29 March 2023/Published online: 31 March 2023.
This article is published with open access at AGH University of Science and Technology Journals.

Abstract

The latest research work in the field of electric power systems focuses on the development of new wire materials which will allow the increase of the transmission capacity of power lines currently in use. The reason for this research was the often limited possibilities of continuous and failure-free transmission of electricity. In this paper, the authors present research on a new aluminium-based alloy dedicated for use as a conductive braid in the HTLS cable group. There are many technical solutions for this group of cables on the market, although they are solutions with a number of disadvantages, ranging from their high price, various operational shortcomings, complicated installation techniques, and ending with the risk of monopolistic practices, which is related to the inability to attract several competitive suppliers. The main aim of the research was to develop a new alloy based on aluminium with the addition of silver and molybdenum dedicated for use in special overhead power cables. Experimental research on new materials focused on obtaining the necessary knowledge to produce an overhead wire from these alloys with higher current carrying capacity in relation to the currently used conventional wire materials based on aluminium.

Keywords:

aluminum, silver, molybdenum, continuous casting, drawing, wire, conductivity, thermal resistance, temperature coefficient of resistance, rheological properties, HTLS conductors

1. INTRODUCTION

Any material dedicated to wire applications should meet a number of requirements, including high electrical and thermal conductivity, high tensile strength and high permissible operating temperature [1–3]. This material should also be corrosion resistant, while the relatively low cost of material used for the conductor is also important [4, 5]. The modern power industry expects new, dedicated aluminum based alloys with non-standard properties, including increased resistance to temperature [6, 7]. Analyzing the examples of solutions patented in recent years, two trends in the field of electric power systems can be observed [8–10]. The first one focuses on the search for high-strength wire materials and the second on the search for alloys with increased thermal resistance, which is closely related to the development of high temperature cables. The thermal resistance of the conductor material is the rate of permanent degradation of the macroscopic strength properties of the material (hardness, tensile strength, yield point) in the work-hardened state as a result of exposure to elevated temperatures. The slower the rate at which the strength properties of the material degrade as a result of increased temperatures proves the higher heat resistance of such a material. Materials with higher heat resistance enable increases in the operating temperature of power cables made from them, thus increasing their current carrying capacity. The most frequently used additive and most widely tested is zirconium, which has a strong influence on increasing the temperature recrystallization of aluminum. There are four types of heat resistance wires made of aluminum-zirconium alloy with working temperatures between 150°C to 230°C without decreasing their properties [11, 12]. The properties of these types of alloys are shown in Table 1.

High-temperature cables are usually bimaterial, with the core of the cable made of steel, invar or a composite, and the conductive layer uses special aluminium alloys with increased heat resistance in the hard state (most often AlZr alloys) or technical purity aluminium after recrystallization [13–17]. Based on research on the synthesis of aluminium alloys with various additives, the addition of silver and molybdenum were selected in order to design a material dedicated for use in overhead power cables [18–22]. Molybdenum, similarly to zirconium, whose effect on increasing the heat resistance of aluminium is widely known, belongs to the group of transition elements. Both metals also belong to the same 5th period of the periodic table, which indicates the similar properties of the two elements. The choice of the silver addition is dictated by its effect on increasing the recrystallization temperature and rheological properties and also reducing the temperature coefficient of resistance after adding it to copper (CuAg alloys) [23–25].

Table 1
Coparison of the properties for standard conductive materials and for higher heat resistance materials [26]

Material	AT1 (Al-Zr)	AT2 (Al-Zr)	AT3 (Al-Zr)	AT4 (Al-Zr)	A1 (Al)
Density [g/cm^3]	2.703	2.703	2.703	2.703	2.703
Resistivity [nΩ·m]	28.735	31.347	28.735	29.726	28.264
Temperature coefficient of resistance [°C^{-1}]	0.00400	0.00360	0.00400	0.00380	0.00403
Tensile strength [MPa]*	159–171	225–248	159–176	159–169	160–200
Elongation [%]*	2.0–1.3	2.0–1.5	2.0–1.5	2.0–1.5	–**
Coefficient of linear expansion [K^{-1}]	23×10^{-6}	23×10^{-6}	23×10^{-6}	23×10^{-6}	23×10^{-6}
Maximum operating temperatures for forty years [°C]	150	150	210	230	80–90
Maximum operating temperatures in 400°C	180	180	240	310	–**

* value depends on the wire cross-section
** non-normalized property

2. MATERIALS AND METHODS

The study was carried out on an aluminium alloy with silver (0.15 wt.%) and one with molybdenum (0.05 wt.%) additives. Cast-rods of 14 mm diameter were obtained using a laboratory workstation for continuous casting. The reference material was high purity aluminium (99.99 wt.%). During the continuous casting process, parameters such as the temperature of the liquid metal, speed, and sequences of continuous casting, conditions of cooling in the crystallizer and macrostructure of ingot were recorded. The continuous casting parameters are presented in Table 2.

The obtained cast-rods were tested in terms of their chemical composition and heat treatment. The chemical composition of Al cast-rods was tested on the SPECTROTEST spectrometer, while the new AlAg0.15Mo0.05 alloy was tested on an emission spectrometer with inductively excited plasma OPTIMA 7300 DV by Perkin Elmer. Materials in an as-cast state and after homogenization were subjected to hardness and electrical conductivity tests. The hardness of the obtained alloys was determined using the Vickers method, the electrical conductivity was carried out using the eddy current method. The obtained bars were drawn to the diameter of the wire rod (ϕ = 9.5 mm), then the homogenization procedure was carried out (temperature 600°C, time 100 h, cooling to water) and then these bars were drawn to the final diameter ϕ = 2.4 mm. Electrical properties, rheological properties and heat resistance of the wires were tested. The electrical properties of the wires were tested at an ambient temperature using the Thomson bridge method. The temperature coefficient of resistance were determined for wires in the deformation-hardened state (after drawing) and in an annealed state (after recrystallization), wires with a diameter of 2.4 mm were placed in the measuring rail of the Thomson bridge and placed in a heating chamber at temperatures of 40, 60, 80 and 100°C (for wires in the recrystallized state, additionally at 120 and 140°C). After the thermal state of the wires was stabilized, their electrical resistance was measured. Accurate reading of the temperature of the wires was possible due to the placement of a thermocouple on the surface of each of them. The measuring base of the wire samples was 0.3 m. From the point of view of the application of the tested materials for the purpose of electric power, a material with high electrical conductivity and a correspondingly low temperature coefficient of resistance has a beneficial effect in increasing the current carrying capacity of the conductor. The next step was to test the stress relaxation of aluminium alloy wires, with the test was carried out at on initial stress level of 100 MPa for 14 h at a stabilized temperature of 21°C, the measuring length of the wire between the jaw clamps was l = 600 mm. The heat resistance test was examined for materials heated at 250°C for the following time intervals: 0.3; 1; 3; 10; 24 and 100 h. The uniaxial tensile test was then carried out on a Zwick Roell Z020 testing machine. The measuring base of the wire was 50 mm, and the test was carried out with a tensile speed of 10 mm/min.

Table 2
The continuous casting parameters of AlAg0.15Mo0.05 and Al cast-rods

Parameter	Al	AlAg0.15Mo0.05
Feed [mm]	10	15
Standstill [s]	10	10
Casting speed [mm/s]	10	10
Liquid metal temperature [°C]	775	811
Cast temperature [°C]	154	168
Water temperature T1* [°C]	7.6	8.3
Water temperature T2** [°C]	13.5	10.9
Primary cooling velocity [min^{-1}]	0.66	0.72
Secondary cooling velocity [min^{-1}]	0.31	0.20

* temperature of the cooling medium before entering the crystallization system
** temperature of the cooling medium after leaving the crystallization system

3. RESULTS AND DISCUSSION

The chemical compositions of the obtained alloy Al99.9 and AlAg0.15Mo0.05 and are presented in Table 3 and Table 4, respectively. The chemical composition of the materials is at the expected level. The actual silver and molybdenum content in the alloys was close to the assumed nominal value, proving that there are no disturbances in the technological process of casting materials.

Table 3
Chemical composition of the Al99.9, wt.%

Al	Si	Fe	Cu	Mn
99.94	0.00486	0.01720	0.01150	0.00127
Mg	Zn	Cr	Ni	Ti
<0.00010	0.00232	0.00557	0.00189	<0.00020
Be	Ca	Li	Pb	Sn
<0.00010	0.00197	0.00013	0.00067	<0.00050
Sr	V	Na	Bi	Zr
0.00101	<0.00050	0.00456	<0.00080	<0.00050
B	Ga	Cd	Co	Ag
0.00022	<0.00040	<0.00010	<0.00020	0.00093
Hg	In	Sb	P	As
<0.0005	<0.0005	<0.0050	<0.0020	<0.0030
Ce	La	Mo		
<0.00100	0.00107	<0.00200		

Table 4
Chemical composition of the AlAg0.15Mo0.05, wt.%

Al	Si	Fe	Cu	Mn
99.74	0.00524	0.01300	0.00690	0.00128
Mg	Zn	Cr	Ni	Ti
<0.00010	0.00071	0.00435	0.00128	0.00020
Be	Ca	Li	Pb	Sn
<0.00010	0.00219	0.00013	0.00113	<0.00050
Sr	V	Na	Bi	Zr
0.00101	<0.00050	0.00416	<0.00080	<0.00050
B	Ga	Cd	Co	Ag
0.00030	<0.00040	<0.00010	0.00023	0.15520
Hg	In	Sb	P	As
<0.00050	0.00086	<0.00500	<0.00200	<0.00300
Ce	La	Mo		
<0.00100	0.00103	0.04900		

The results of the Vickers hardness and electrical conductivity tests are shown in Figures 1 and 2. On the basis of the results obtained for the samples in the as-cast condition, there is an increase in hardness for the aluminium alloy with Ag and Mo additions (20 HV5) compared to the reference aluminium sample (18 HV5). After homogenization, the hardness of the AlAg0.15Mo0.05 slightly decreased to 19.7 HV5. Molybdenum in the tested amount may be located, depending on the conditions of heat treatment, in a solid solution or in a separate phase. Based on the Al-Ag and Al-Mo binary equilibrium systems and on the results of the electrical conductivity tests, it is postulated that both components are deposited in an aluminium solid solution after homogenization. The heat treatment slightly lowers the electrical properties of the material. AlAg0.15Mo0.05 alloy in the as-cast state generally have acceptable electrical properties (their resistivity does not exceed the level of 29 nΩ·m), although the electrical conductivity of the ternary alloy is slightly above the expected maximum limit. Heat treatment causes a slight decrease in the electrical properties of the material.

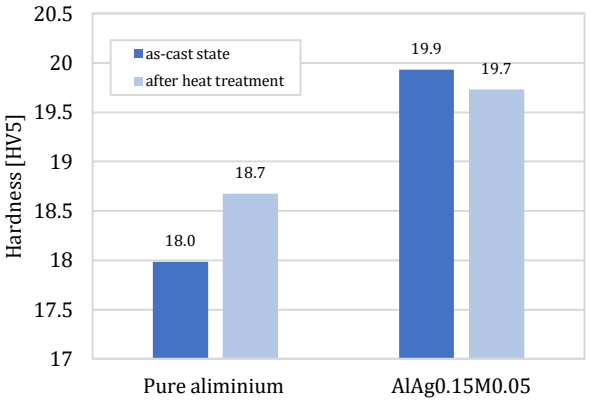

Fig. 1. Vickers hardness results in the as-cast state and after heat treatment (homogenization and cooling to water) of the AlAg0.15M0.05 alloy

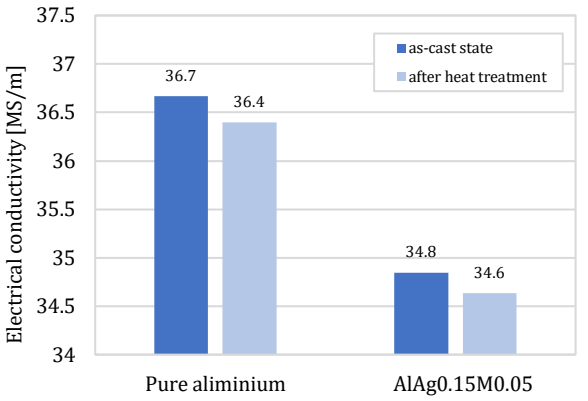

Fig. 2. Results of the electrical conductivity in the as-cast state and after heat treatment (homogenization and cooling to water) of the AlAg0.15M0.05 alloy

Table 5 shows the results of the tested electrical properties of aluminium alloy wires in the deformation-hardened state (after drawing). Electrical properties of heat-resistant wires AlZr type AT1 according to Table 1 are at the level of 28.735 nΩ·m (before the drawing process, this value oscillates around the level of 28.1 nΩ·m), while the resistivity of the new alloy AlAg0.15M0.05 is higher than expected and amounts to 29.48 nΩ·m.

Table 5
Electrical properties of the wire

Alloy	Resistivity [nΩ·m]	Electrical conductivity [MS·m^{-1}]	IACS [%]
Al	27.96	35.77	61.67
AlAg0.15Mo0.05	29.48	33.93	58.49

Figures 3 and 4 show the results of the temperature coefficient of wire resistance test for both materials, while the test results are summarized in Table 6. The angle of slope of the line is the temperature coefficient of resistance. Based on the research, it is worth noting that the synergistic effect of Ag and Mo allowed the temperature coefficient of resistance to be reduced by approx. 10%. This is a reduction that is beneficial from a utilitarian point of view.

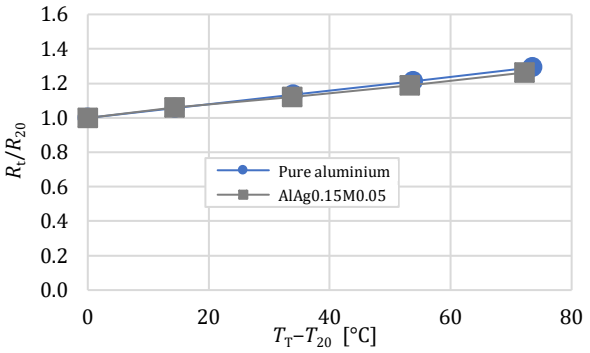

Fig. 3. Temperature coefficient of resistance of the tested materials in the deformation-hardened state

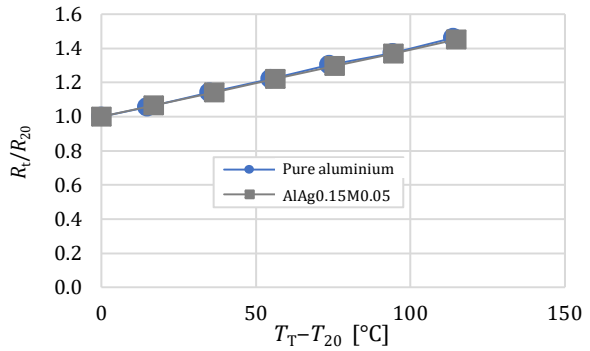

Fig. 4. Temperature coefficient of resistance of the tested materials in the annealed state

Table 6
Temperature coefficient of resistance of the tested materials in the deformation-hardened/annealed state

Alloy	Temperature coefficient of resistance [K⁻¹] (deformation--hardened state)	Temperature coefficient of resistance [K⁻¹] (annealed state)
Al	0.0040	0.0041
AlAg0.15Mo0.05	0.0036	0.0039

Figure 5 presents the results of the thermal resistance test of wires in a graphic form, while the obtained values are also summarized in Table 7.

The tensile strength of the deformation-hardened wires is respectively 116 MPa for the aluminium wire and 120 MPa for the AlAg0.15Mo0.05 wire, which shows a significantly higher stability of the strength properties. The AlAg0.15Mo0.05 alloy shows significantly higher stability in terms of strength properties, after holding at 250°C for 100 h, it showed a decrease in tensile strength by 17% (100 MPa) compared to the wire in the hard state (120 MPa). The reference aluminium wire with a purity of 99.9% is characterized by a decrease in strength properties by 24%. The achieved result proves the significantly higher heat resistance of the developed three-component aluminium alloy compared to the reference aluminium. Therefore, it can be concluded that the AlAg0.15Mo0.05 wires show about a 1.5 times lower strength decrease compared to pure aluminium wires.

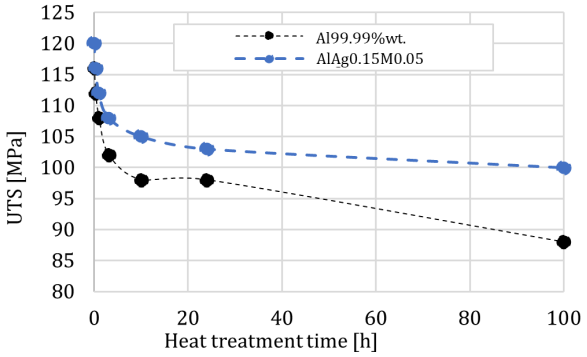

Fig. 5. Thermal resistance of Al99.99%wt. and AlAg0.15Mo0.05 wires

Table 7
Thermal resistance of Al99.99%wt. and AlAg0.15Mo0.05 wires

Heat treatment time [h]	Material	
	Al	AlAg0.15Mo0.05
	UTS [MPa]	
0	116	120
0.3	112	116
1	108	112
3.1	102	108
10	98	105
24	98	103
100	88	100

Figure 6 shows the stress relaxation of the aluminium alloy wires test results. The relaxation test was carried out at on initial stress level of 100 MPa, the test was carried out for 14 h at a stabilized temperature of 21°C, the measuring length of the wire between the jaw clamps was l = 600 mm. The obtained test results showed the higher rheological resistance of the AlAg0.15Mo0.05 alloy wires than wires made of pure aluminium.

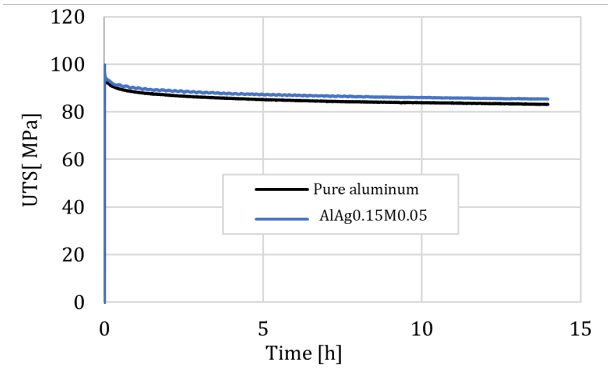

Fig. 6. Stress relaxation test results

4. CONCLUSIONS

Currently, the braids of high-temperature cables are made of aluminium-zirconium alloys, with four types of such wires having been developed so far (AT1-AT4). These alloys are a solution to current electricity problems – they allow for a significant increase in the transmission capacity of power lines. The addition of zirconium increases the heat resistance of aluminium by increasing its recrystallization temperature (heat-resistant AlZr alloys allow for the working temperature of the wires to be increased up to 230°C), while the permissible long-term working temperature of commonly used aluminium and steel-aluminium wires is +80°C. AlZr alloys, despite many advantages, also have a number of drawbacks, ranging from their high price, various operational shortcomings, complicated installation techniques, and ending with the risk of monopolistic practices, which is associated with the inability to acquire several competing suppliers. It is these shortcomings, together with the deficit of the transmission capacity of the currently used systems, that have become the inspiration to look for new, alternative aluminium-based alloys in recent years that will be able to meet the growing operational requirements.

As part of the research, alloys with nominal alloying additions of silver (0.15 wt.%) and molybdenum (0.05 wt.%) were produced by continuous casting in laboratory conditions with the use of 99.9% pure aluminium matrix (this aluminium was also produced as a reference material). The quality of the castings was satisfactory. The tested materials in the as-cast state generally have acceptable electrical properties (their resistivity does not exceed 29 nΩ·m), although the electrical conductivity of the ternary alloy is slightly above the expected maximum – the preferred value in the pre-drawing condition is a maximum of 28.1 nΩ·m (as for AT1 reference material). No effective increase in the strength properties of the material was observed due to the addition of Mo and Ag in the tested range in the as-cast state, although a similar situation occurs in the case of the high-temperature AlZr alloys – AT1 and AT3, which are used in practice. The heat resistance of the wires with the addition of Mo and Ag is higher than pure aluminium wire, it can be postulated that this resistance is comparable to the heat resistance of AlZr0.05 (AT1). Alloy additions in the form of silver and molybdenum lower the temperature coefficient of resistance, which reduces the increase in the resistance of the conductor along with its temperature increase resulting from the heat balance, allowing a favourable current carrying capacity of the target high-temperature conductor to be achieved. The lower temperature coefficient of the AlAgMo material resistance in the annealed state compared to aluminium wire has potential advantages from the point of view of using such material in low-sag high-temperature ACSS cables, where the braid is made of recrystallized aluminium. The developed AlAg0.15Mo0.05 alloy shows higher rheological resistance than pure aluminium. On the basis of the conducted research, it is possible to design an AlAgMo alloy with a resistivity similar to AlZr (AT1) wires currently used for high temperature low sag conductors.

Cables made of the new alloy AlAg0.15Mo0.05 would enable the increase of their current carrying capacity and the operation of cables at elevated temperatures without the risk of the degradation of their strength properties. Based on the knowledge obtained during the research, it is possible to design a high-temperature cable with a braid made of the new material and to simulate its operation in an overhead power line.

REFERENCES

[1] Zhang C. & Chen R. (2013). Patent No. CN103014462 A. China, The State Intellectual Property Office of People's Republic of China.
[2] Gaofeng W. (2013). Patent No. CN103021500 A. China, The State Intellectual Property Office of People's Republic of China.
[3] Central South University (2013). Patent No. CN102965550 A. China, The State Intellectual Property Office of People's Republic of China.
[4] Daimin Cable Ltd. (2013). Patent No. CN102978491 A. China, The State Intellectual Property Office of People's Republic of China.
[5] Furukawa Electric Co. Ltd. (2013). Patent No. EP2597169 A1. Munich, Germany, European Patent Office.
[6] Misato K., Yoshihiro N., Taichirou N., Yoshiyuki T. & Yasuyuki O. (2014). Patent No. US 8653374. United States Patent and Trademark Office.
[7] Siripurapu S., Muojewu C., Sekunda J., Baker R., Duer N. & Vo N. (2017). Patent No. WO/2017/066638. Canadian Patent Application.
[8] Siripurapu S., Muojewu C., Sekunda J., Baker R., Duer N. & Vo N. (2019). Patent No. US20170110704 A1. United States Patent Application Publication.
[9] Net. Sci. Ltd. (2020). Patent No. CN110791685 A. China, The State Intellectual Property Office of People's Republic of China.
[10] Wuhan Cable Ltd. (2020). Patent No. CN110669951 A. China, The State Intellectual Property Office of People's Republic of China.
[11] Knych T. (2010). *Elektroenergetyczne przewody napowietrzne. Teoria – materiały – aplikacje*. Kraków: Wydawnictwa AGH.
[12] Uliasz P. (2010). *Dobór materiału i opracowanie konstrukcji wysokotemperaturowych przewodów elektroenergetycznych ze stopów AlZr* [doctoral dissertation]. AGH University of Science and Technology.
[13] Koike K. (1966). Patent No. US3278300. United States Patent Office.
[14] Iricibar R., Pampillo C. & Chia U. (1980). Metallurgical aspects of aluminium alloys for electrical applications. In: Embury D.E., Pampillo C.A. & Biloni H., *Aluminium Transformation Technology and Applications: Proceedings of the International Symposium at Puerto Madryn, Chubut, Argentine, August 21–25, 1978*, 241–303.
[15] Kenji M. & Toshiya I. (2000). Patent No. EP0787811 B1. European Patent Application.
[16] Matsuda Y., Yokota M. & Okumura T. (1972). Traces of Yttrium in ACSR aluminium boosts transmission efficiency 50%. Wire Journal, #P02831. Retrieved from https://portal.wirenet.org/ [accessed: 28.10.2022].
[17] Knych T., Mamala A., Grzebinoga J., Kwaśniewski P., Ściężor W., Kiesiewicz G., Gniełczyk M. & Kowal R. (2015). Badania wpływu dodatku chromu do aluminium na własności mechaniczne i elektryczne drutów AlCr. *Hutnik. Wiadomości Hutnicze*, 1(82), 59–63. Doi: https://doi.org/10.15199/24.2015.1.12.
[18] Mamala A., Kowal R., Kwaśniewski P., Knych T., Ściężor W., Kiesiewicz G., Gniełczyk M. & Grzebinoga J. (2015). Badania wpływu dodatku wapnia do aluminium na własności mechaniczne i elektryczne stopów Al-Ca. *Hutnik. Wiadomości Hutnicze,* 82(1), 81–84. Doi: https://doi.org/10.15199/24.2015.1.17.
[19] Grzebinoga J., Mamala A., Knych T., Kwaśniewski P., Ściężor W., Kiesiewicz G., Kawecki A., Sieja-Smaga E. & Jurkiewicz B. (2016). New aluminium base materials for use on electrical purposes. *Key Engineering Materials*, 682, 61–68. Doi: https://doi.org/10.4028/www.scientific.net/KEM.682.61.
[20] Mamala A., Grzebinoga J., Kowal R., Ściężor W., Jabłoński M. & Gniełczyk M. (2017). Własności reologiczne nowych stopów na bazie aluminium dedykowanych do zastosowań na cele elektryczne. *Rudy i Metale Nieżelazne Recykling*, 7(62). Doi: https://doi.org/10.15199/67.2017.7.2.

[21] Snopiński P., Matus K., Taticek F. & Rusz S. (2022). Overcoming the strength-ductility trade-off in additively manufactured AlSi10Mg alloy by ECAP processing. *Journal of Alloys and Compounds*, 918, 165817. Doi: https://doi.org/10.1016/j.jallcom.2022.165817.

[22] Maziarz W., Greger M., Długosz P., Dutkiewicz J., Wójcik A., Rogal Ł., Stan-Głowińska K., Hilser O., Pasternak M., Cizek L. & Rusz S. (2022). Effect of severe plastic deformation process on microstructure and mechanical properties of AlSi/SiC composite. *Journal of Materials Research and Technology,* 17, 948–960. Doi: https://doi.org/10.1016/j.jmrt.2022.01.023.

[23] Kawecki A., Sieja-Smaga E., Knych T., Mamala A., Kwaśniewski P., Kiesiewicz G. & Ichas K. (2015). Badania wpływu parametrów obróbki cieplnej i przeróbki plastycznej na optymalizację własności elektrycznych drutów ze stopu CuAg5. *Hutnik. Wiadomości Hutnicze*, 82(1), 51–54. Doi: https://doi.org/10.15199/24.2015.1.10.

[24] Kawecki A., Knych T., Sieja-Smaga E., Mamala A., Kwaśniewski P., Kiesiewicz G. & Pacewicz A. (2013). Badania wpływu ciągnienia i obróbki cieplnej na własności wytrzymałościowe i elektryczne drutów ze stopów CuAg5 i CuAg15 z linii ciągłego topienia i odlewania. *Hutnik. Wiadomości Hutnicze*, 80(1), 47–50.

[25] Sieja-Smaga E., Kawecki A., Knych T., Kiesiewicz G. & Kwaśniewski P. (2013). Analiza zmian odporności cieplnej stopów Cu-Ag z przeznaczeniem na wyroby branży elektroenergetycznej. *XLI Szkoła Inżynierii Materiałowej*: *24–27 września. Kraków – Krynica.* Wydawnictwo Naukowe AKAPIT, 434–438.

[26] Yaojun M., Feng Z., Xiaolin M., Chunjian X. & Xiaohong H. (2009). Patent No. CSN EN 62004. China, The State Intellectual Property Office of People's Republic of China.